(Received 5 November 2025, Accepted 28 January 2026, Scheduled 10 February 2026)

Wide-Passband Miniaturized Filter with Higher-Order Mode Suppression Using QMSIW and Microstrip Resonators

Jingyv Wang, Haiyan Zeng, Mengling Su, Xuan'an Chen, Lishan Huang, Jinming Ou, and Xiaohei Yan*

School of Physics and Electronic Information Engineering, Guangxi Minzu Normal University, Chongzuo 532200, China

ABSTRACT: This paper presents a wide-passband, miniaturized filter based on quarter-mode substrate-integrated waveguide (QMSIW) resonant cavities and microstrip resonators. The filter employs two QMSIW resonant cavities, which effectively reduce its size. Moreover, the higher-order modes TE_{120}, TE_{210}, and TE_{220} cannot propagate within these cavities. The addition of two microstrip resonators at the coupling iris between the QMSIW cavities enables a fourth-order filter response using only two resonant cavities. High selectivity is achieved through cross-coupling, which introduces two transmission zeros (TZs). The filter was fabricated and measured, showing good agreement with the simulation results. Compared with other substrate-integrated waveguide (SIW) filters, the proposed filter offers advantages in compactness, passband bandwidth, and higher-order mode suppression.

1. INTRODUCTION

Filters play a pivotal role in communication systems by selectively passing or suppressing specific frequency components of signals to achieve spectral shaping, noise suppression, and distortion reduction, thereby enhancing transmission quality and system reliability. Substrate-integrated waveguides (SIWs) exhibit several advantageous characteristics, including low insertion loss, high-quality factor (Q), low fabrication cost, and ease of integration with planar circuits. These attributes have contributed to their widespread adoption in filter design, as evidenced by their frequent use in numerous studies [1–5]. However, SIW filters generally occupy a larger circuit area than microstrip filters. Moreover, because SIWs support mode characteristics similar to those of conventional rectangular waveguides, their higher-order mode spectra are densely spaced, resulting in spurious resonances closer to the passband.

In recent years, some researchers have proposed hybrid bandpass filters that combine the advantages of substrate-integrated waveguide (SIW) resonant cavities with those of microstrip resonators. This approach has the potential to overcome certain limitations of SIW-based filters. In [6], a hybrid-structured bandpass filter (BPF) was proposed, integrating a full-size SIW resonant cavity with a microstrip line resonator. The filter exhibits excellent performance, including sharp skirt selectivity and low insertion loss. However, its physical size remains relatively large. In [7], a single-layer, fourth-order bandpass filter was introduced by coupling two SIW cavities with two folded quarter-wavelength microstrip line resonators. Nevertheless, reliance on SIW resonator cavities limits miniaturization. In [8], a BPF with wide stopband characteristics was realized by etching two microstrip-based uniform-impedance resonators (UIRs) between two SIW cavities. The staggered higher-order mode frequencies of the UIRs and SIWs help suppress harmonics generated by both resonant structures. However, the filter still exhibits a relatively large circuit size. In [9], a novel filter with high selectivity was proposed using a hybrid multilayer half-mode substrate-integrated waveguide (HMSIW) structure. Although the circuit size was reduced, the structure became more complex, and the double-layer configuration increased the overall volume of the filter. These drawbacks may limit its practical applicability. In [10], a miniaturized multilayer quarter-mode substrate-integrated waveguide (QMSIW) filter with high selectivity and a wide stopband was proposed. The QMSIW structure significantly reduces the circuit size; however, its dual-layer configuration still renders the filter complex and difficult to fabricate. In [11], a wideband BPF was proposed by embedding a multimode resonator (MMR) in a single-SIW cavity. This filter exhibits a relatively wide passband. However, it employs a multilayer structure, and both the selectivity on the lower-frequency side of the passband and the return loss within the passband are suboptimal. Ref. [12] proposes a novel, compact BPF based on a self-packaged hybrid structure combining SIW and stripline technologies. The proposed filter realizes an equivalent box-like coupling scheme, enabling the generation of three finite transmission zeros (FTZs). Nevertheless, its multilayer architecture increases insertion loss and limits practical applicability.

The research on the design of miniaturized hybrid-structured filters is still in its nascent stage. Further investigation in this field holds great scientific and practical significance. Accordingly, this paper proposes a hybrid-structure bandpass filter (BPF) based on quarter-mode substrate-integrated waveguide (QMSIW) cavities and microstrip resonators. First, the use of QMSIW cavities effectively reduces the filter's size. Moreover, the higher-order modes TE_{120}, TE_{210}, and TE_{220} cannot propagate within the resonant cavity, thereby significantly widening

* Corresponding author: Xiaohei Yan (yanxiaohei@gxnun.edu.cn).

the stopband. Second, two microstrip resonators are embedded at the coupling iris, enabling the realization of a fourth-order filter response using only two resonant cavities. Concurrently, two transmission zeros (TZs) are introduced via cross-coupling to ensure high selectivity. Finally, the filter features a single-layer structure, facilitating fabrication and integration into communication systems.

2. STRUCTURE AND COUPLING TOPOLOGY OF THE FILTER

In this design, a single-layer substrate-integrated waveguide cavity structure is employed, and its three-dimensional structure is depicted in Figure 1(a). The structure comprises two metal layers and one dielectric layer. The dielectric layer is composed of ZYF300CA-P, which exhibits a relative permittivity of 3, a loss tangent of 0.0018, and a thickness of 0.762 mm. Figure 1(b) depicts the dimensions of the upper metal layer of the filter. The filter comprises two QMSIW resonant cavities, which operate in $TE_{0.5/0.5/0}$ mode. A coupling iris is situated at the common edge of the two resonant cavities, and two microstrip resonators are embedded within the coupling iris. The microstrip resonators may be considered equivalent to quarter-wavelength short-circuit resonators. A pair of metal through-holes are situated on the lower side of the microstrip resonators.

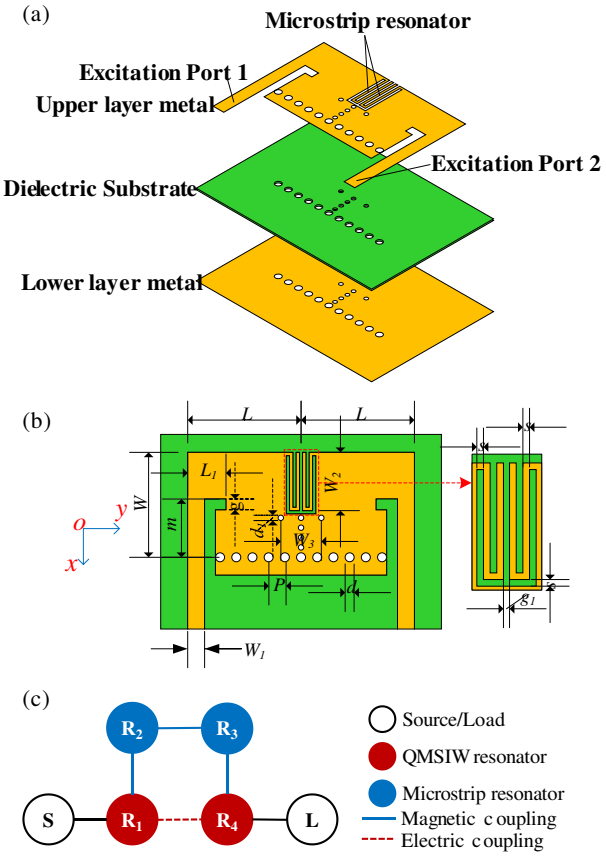

FIGURE 1. (a) Structure of the filter; (b) Dimensioned view of the upper metal layer of the filter; (c) Coupling topology of the filter. (Physical dimensions (mm): $L = 12.6$, $P = 1.8$, $d = 1$, $W = 11.7$, $W_1 = 1.88$, $L_1 = 4.25$, $m = 6.5$, $g = 1.2$, $d_1 = 0.6$, $W_2 = 6.5$, $W_3 = 4.5$, $g_1 = 0.34$, $s = 0.37$).

The coupling between the QMSIW cavity and microstrip resonators can be adjusted by the dimension W_3. The coupling between the two microstrip resonators can be adjusted by the spacing g. The input and output ports are equipped with a 50-ohm coplanar waveguide, which facilitates energy coupling between the source or load and the filter.

The coupling topology of the filter, based on its structural characteristics, is depicted in Figure 1(c). The coupling between the QMSIW cavity and the microstrip resonator is magnetic in nature. The short-circuited ends of the two microstrip resonators are in close proximity, thereby establishing a magnetic coupling between them. The electrical coupling between the two QMSIW cavities is relatively weak because a portion of the electric field can be coupled through the open edges of the cavities. The electrical coupling between the QMSIW cavities is responsible for the cross-coupling, which in turn generates transmission zeros on both sides of the filter's passband. This improves the selectivity of the filter.

3. FILTER DESIGN AND PRINCIPLE ANALYSIS

3.1. Determination of QMSIW Resonant Cavity Size and Microstrip Resonator Size

The quarter-mode substrate-integrated waveguide (QMSIW) resonant cavity can be regarded as being obtained by making two cuts along the planes of symmetry of the SIW cavity, whose dimensions are 1/4 of those of the SIW cavity. The resonance frequency of the main mode $TE_{0.5/0.5/0}$ of the QMSIW resonant cavity is determined by the TE_{110} mode of the SIW cavity. The resonance frequency of the TE_{110} mode of the SIW cavity is calculated using Equation (1):

$$f_{TE_{101}} = \frac{c_0}{2\sqrt{\varepsilon_r}} \sqrt{\left(\frac{1}{W_{eff\text{-}SIW}}\right)^2 + \left(\frac{1}{L_{eff\text{-}SIW}}\right)^2} \quad (1)$$

where c_0 is the speed of light in vacuum; ε_r is the relative permittivity of the dielectric substrate; and $W_{eff\text{-}SIW}$ and $L_{eff\text{-}SIW}$ are the equivalent width and length of the SIW cavity, which are defined as follows:

$$\begin{aligned} W_{eff\text{-}SIW} &= W_{SIW} - \frac{d^2}{0.95P}, \\ L_{eff\text{-}SIW} &= L_{SIW} - \frac{d^2}{0.95P} \end{aligned} \quad (2)$$

where W_{SIW} and L_{SIW} denote the width and length of the SIW cavity, respectively. The diameter of the circular holes is designated as d, and the center distance between adjacent circular holes is designated as p. In this design, the values of W_{SIW} and L_{SIW} are equal to $2W$ and $2L$, respectively.

Given that the microstrip resonator can be considered equivalent to a quarter-wavelength short-circuited resonator [8], its input susceptance can be expressed as $Y_{\text{in}} = -jY_0\cot\theta_0$. When Y_{in} is equal to zero, the equation for the resonance frequency can be expressed as:

$$f_i = \frac{c_0}{\sqrt{\varepsilon_e}} \frac{1+2i}{4l_R} \quad (3)$$

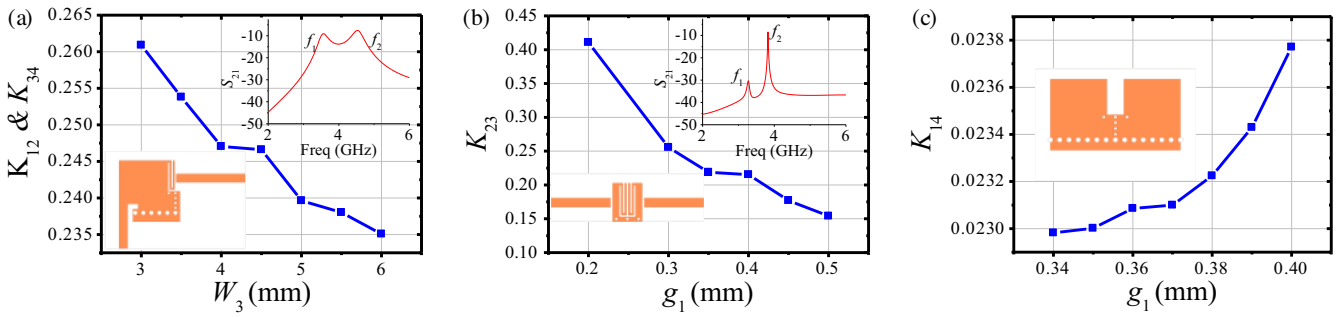

FIGURE 2. (a) Extracted coupling coefficients K_{12} and K_{34} versus the dimension W_3. (b) K_{23} versus the dimension g_1. (c) K_{14} versus the dimension g_1.

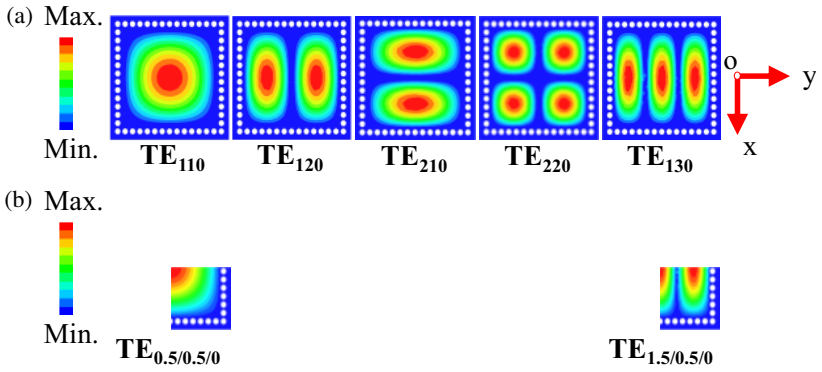

FIGURE 3. (a) Electric field strength distribution of some modes in the SIW cavity; (b) Electric field strength distribution of some modes in the QMSIW cavity.

where ε_e is the equivalent dielectric constant of the microstrip resonator, and l_R is the length of the resonator. $i = 0, 1, 2, \ldots$, when $i = 0$, it denotes the main resonant mode, and when $i > 0$, it denotes the higher-order resonant mode.

Consequently, once the design frequency of the filter has been determined, the initial design of the QMSIW cavity and microstrip resonator can be carried out.

3.2. Specifications and Design Curves

As an illustrative example, the proposed filter is synthesized with a fourth-order quasi-elliptic response centered at 4.12 GHz, exhibiting a 21-dB return loss and a 32.7% relative bandwidth. The coupling matrix parameters can be synthesized according to the procedure outlined in [13]. The resulting coupling coefficients and external quality factors are as follows:

$$\begin{aligned} K_{12} &= K_{34} = 0.3, \quad K_{23} = 0.24, \\ K_{14} &= -0.023, \quad Q_e = 2.76 \end{aligned} \tag{4}$$

In this context, K_{ij} represents the coupling coefficients between the resonators R_i and R_j, while Q_e is the external quality factor. As illustrated in Figure 2, the main coupling coefficients (i.e., K_{12} and K_{34}, K_{23}) can be extracted in the case of weak external coupling. The corresponding simulation models and transfer responses are shown in the inset. Figure 2(a) illustrates that K_{12} and K_{34} decrease with the enlargement of W_3, as electromagnetic signals are more likely to be shorted to the ground with the increase of W_3. With regard to K_{23}, there is a notable decline in its value from 0.411 to 0.154 as the gap (i.e., g_1) increases from 0.2 to 0.5 mm. The cross-coupling coefficient K_{14} is extracted by eigenmode simulation, as illustrated in Figure 2(c). This coefficient is primarily influenced by the dimension g_1. As illustrated, K_{14} exhibits an increase from 0.0230 to 0.0238 in conjunction with an enlarged g_1. All these extracted curves are instructive for filter design, although some numerical deviations may exist compared to the synthesized parameters.

3.3. Suppression of Higher-Order Modes

Due to the high aspect ratio of the SIW (typically greater than 10), when the SIW cavity is sliced along the symmetry plane, the energy is mainly confined to propagate in the semi-open dielectric-filled region surrounded by the metal through-hole arrays and the upper and lower metal planes. The open side may be regarded as an ideal magnetic wall, so that the primary mode electric field distribution of the QMSIW cavity will be essentially unaltered, with only one-quarter of the electric field of the SIW cavity retained. Similarly, for the higher-order modes of the QMSIW cavity, they can propagate within the cavity only if they are equivalent to magnetic walls at the symmetry planes. Figure 3(a) depicts the first five resonant modes of the SIW cavity. Figure 3(b) depicts the first two resonant modes of the QMSIW cavity. It can be observed that the higher-order modes, TE_{120}, TE_{210}, and TE_{220}, which cannot be equated to magnetic

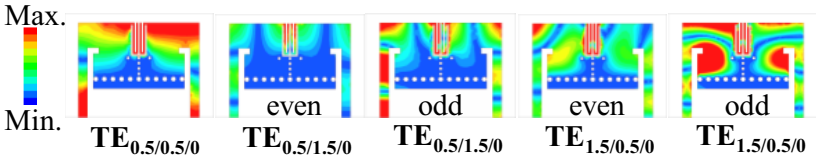

FIGURE 4. Electric field strength distribution of some modes in the filter.

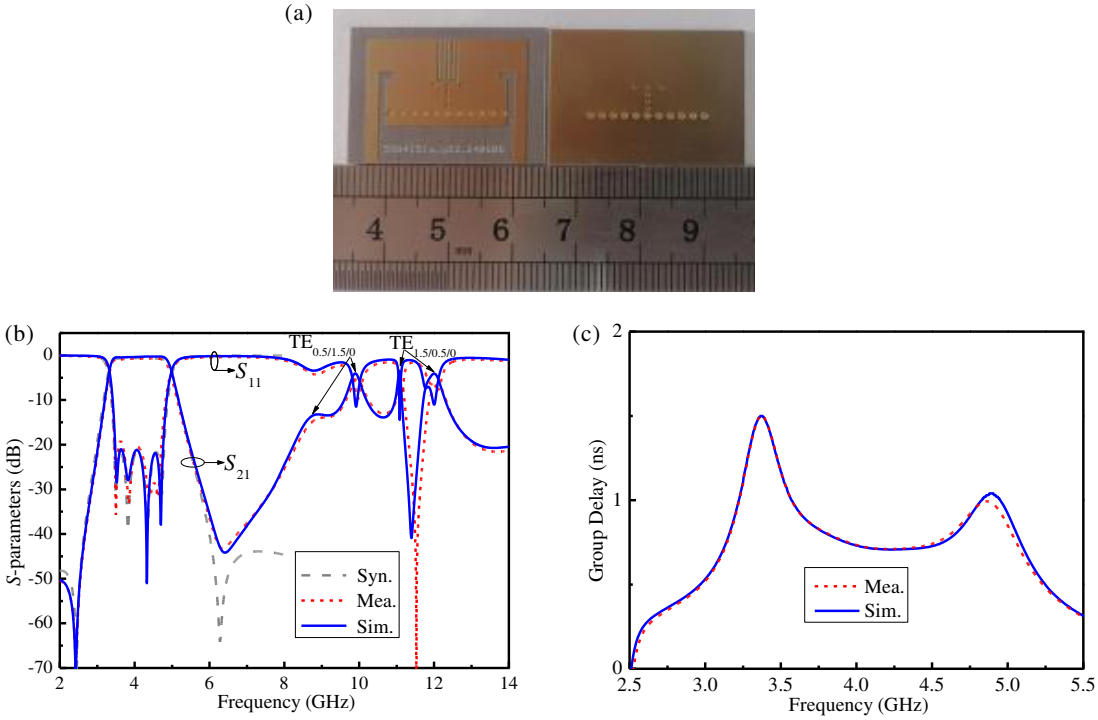

FIGURE 5. (a) Physical diagram of the filter; (b) synthesized, measured, and Simulated S-parameters of the filter; (c) group delay curves of the filter.

walls at the symmetry planes, are suppressed, and this suppression can be achieved by employing the structural characteristics of the QMSIW.

Figure 4 depicts the electric field distribution of the main mode, $TE_{0.5/0.5/0}$, and the two higher-order modes, $TE_{0.5/1.5/0}$ and $TE_{1.5/0.5/0}$, which are situated closest to the passband in the filter. It can be observed that the primary mode, $TE_{0.5/0.5/0}$, is capable of propagating through the filter in a manner consistent with its intended functionality. The higher-order modes $TE_{0.5/1.5/0}$ and $TE_{1.5/0.5/0}$ both split into pairs of odd and even modes, which produce specific responses in the filter and form parasitic passbands. The parasitic passbands generated by modes corresponding to the higher-order modes TE_{120}, TE_{210}, and TE_{220} of the SIW cavity are not observed in the filter, which supports the preceding discussion.

4. FABRICATION, TESTING, AND DISCUSSION

To verify the performance of the aforementioned filter, it was fabricated using the printed circuit board (PCB) process. Figure 5(a) depicts the physical diagram of the fabricated filter, which has a physical size of $25.2 \times 11.7\,\text{mm}^2$ (excluding the input and output ports). To test the filter, SMA-KHD coaxial connectors were soldered to the input and output ports, and the filter was connected to an Agilent vector network analyzer (E8363C) for measurement. Figure 5(b) shows the simulated, synthesized, and measured S-parameters over the frequency range from 2 to 14 GHz. There is good agreement between the simulated and measured results. However, the measured center frequency of 4.1 GHz is slightly lower than the simulated value. The measured 3 dB fractional bandwidth (FBW) is 39.47%, with a minimum insertion loss (including the loss from the SMA connectors) of 0.9 dB. Furthermore, the stopband extends up to 8.25 GHz, with a rejection level exceeding 20 dB. As anticipated, two transmission zeros are observed on either side of the passband. The measured insertion loss is 0.5 dB higher than the simulated value, while the return loss is better than 19 dB (which is 2 dB lower than the simulated value). Figure 5(c) displays the group delay curves of the filter. It is evident that the group delay of the filter is less than 1.5 ns in the passband, and the maximum group delay variation is only 0.8 ns. The discrepancy between the measured and simulated results is primarily attributable to processing errors, dielectric loss, and transition structure losses.

A comparison of the proposed filter with other reported works is presented in Table 1. The results demonstrate that the proposed filter exhibits superior performance in terms of relative bandwidth, insertion loss, return loss, and size compared

TABLE 1. Comparison with similar filters in the literature.

Refs.	[6]	[7]	[8]	[9]	[10]	[11]	[12]	This work
F_0 (GHz)	11.5	9.7	10.1	10.7	8.88	26.7	10.1	4.1
FBW (%)	6.78	12	11.7	10	17.7	34.8	11.6	39.47
IL (dB)	1.42	0.9	1.22	1.57	1.29	0.6	1.67	0.9
RL (dB)	13	15	15	15	18	13	15	19
Order	4	4	4	4	4	3	4	4
No. of TZs	2	2	2	2	2	2	3	2
Layer	1	1	1	2	2	3	2	1
size ($\lambda_g \times \lambda_g$)	0.91×0.56	\	0.54×0.93	0.84×0.45	0.35×0.53	0.37×0.37	1.35×0.67	0.34×0.16

with other hybrid-structure filters. Moreover, the filter has a single-layer structure, which is straightforward to fabricate and integrate into communication systems.

5. CONCLUSION

This paper presents a novel hybrid-structure filter that combines microstrip and quarter-mode substrate-integrated waveguide (QMSIW) technologies. The filter features a wide passband. The incorporation of QMSIW cavities not only reduces the filter's physical size but also broadens the stopband by suppressing the propagation of certain higher-order modes within the resonant cavities. Integrating two microstrip resonators inside the QMSIW cavities enables a fourth-order response, yielding a more compact design. Furthermore, cross-coupling is introduced to generate transmission zeros (TZs) on both sides of the passband, thereby enhancing the filter's selectivity. The filter's wide passband, low insertion loss, and small size make it an optimal choice for high-performance communication systems.

ACKNOWLEDGEMENT

This work is supported by the Chongzuo Science and Technology Program Project (No. 2025ZC0713), the School-level Research Project of Guangxi Minzu Normal University (No. 2024FW028) and the Guangxi University Student Innovation and Entrepreneurship Training Program Project (No. 202510604011).

REFERENCES

[1] Jia, D., Q. Feng, Q. Xiang, and K. Wu, "Multilayer substrate integrated waveguide (SIW) filters with higher-order mode suppression," *IEEE Microwave and Wireless Components Letters*, Vol. 26, No. 9, 678–680, Sep. 2016.

[2] Zhou, K., C.-X. Zhou, and W. Wu, "Resonance characteristics of substrate-integrated rectangular cavity and their applications to dual-band and wide-stopband bandpass filters design," *IEEE Transactions on Microwave Theory and Techniques*, Vol. 65, No. 5, 1511–1524, May 2017.

[3] Zhang, Y.-C., J.-Q. Ge, and G.-A. Wang, "Enabling electrically tunable radio frequency components with advanced microfabrication and thin film techniques," *Journal of Central South University*, Vol. 29, No. 10, 3248–3260, 2022.

[4] Huang, Y. M., W. Jiang, H. Jin, Y. Zhou, S. Leng, G. Wang, and K. Wu, "Substrate-integrated waveguide power combiner/divider incorporating absorbing material," *IEEE Microwave and Wireless Components Letters*, Vol. 27, No. 10, 885–887, Oct. 2017.

[5] Jiang, W., W. Shen, T. Wang, Y. M. Huang, Y. Peng, and G. Wang, "Compact dual-band filter using open/short stub loaded stepped impedance resonators (OSLSIRs/SSLSIRs)," *IEEE Microwave and Wireless Components Letters*, Vol. 26, No. 9, 672–674, Sep. 2016.

[6] Lin, G. and Y. Dong, "A compact, hybrid SIW filter with controllable transmission zeros and high selectivity," *IEEE Transactions on Circuits and Systems II: Express Briefs*, Vol. 69, No. 4, 2051–2055, Apr. 2022.

[7] Lu, Z. and Y. Dong, "A compact SIW bandpass filter embedded with folded quarter-wavelength resonators," in *2022 International Conference on Microwave and Millimeter Wave Technology (ICMMT)*, 1–3, Harbin, China, 2022.

[8] Zhu, Y. and Y. Dong, "A novel compact wide-stopband filter with hybrid structure by combining SIW and microstrip technologies," *IEEE Microwave and Wireless Components Letters*, Vol. 31, No. 7, 841–844, Jul. 2021.

[9] Gu, L. and Y. Dong, "Compact half-mode SIW filter with high selectivity and improved stopband performance," *IEEE Microwave and Wireless Components Letters*, Vol. 32, No. 9, 1039–1042, Sep. 2022.

[10] Lin, G., Y. Dong, and X. Luo, "Miniaturized quarter-mode SIW filters loaded by dual-mode microstrip resonator with high selectivity and flexible response," *IEEE Microwave and Wireless Components Letters*, Vol. 32, No. 6, 660–663, Jun. 2022.

[11] He, X., D. Ding, and X. Y. Zhang, "An SIW-based wideband 5G mmWave bandpass filter by using multimode resonator," *IEEE Microwave and Wireless Technology Letters*, Vol. 35, No. 4, 412–415, Apr. 2025.

[12] Fan, C., Y. Hao, K. Gong, Y. Liu, J. Sun, Q. Liu, and Y. Liu, "Compact self-packaged hybrid SIW bandpass filters with controllable finite transmission zeros," *IEEE Microwave and Wireless Technology Letters*, Vol. 35, No. 6, 682–685, Jun. 2025.

[13] Chu, P., L. Guo, L. Zhang, F. Xu, W. Hong, and K. Wu, "Wide stopband substrate integrated waveguide filter implemented by orthogonal ports' offset," *IEEE Transactions on Microwave Theory and Techniques*, Vol. 68, No. 3, 964–970, Mar. 2020.